KERNFORSCHUNGSANLAGE JÜLICH GmbH
Institut für Reaktorentwicklung

Reactor Physics Concept for a Low Enriched Compact Core

by

Hartwig Schaal
Istvan Vidovszky

Jül-2116
February 1987
ISSN 0366-0885

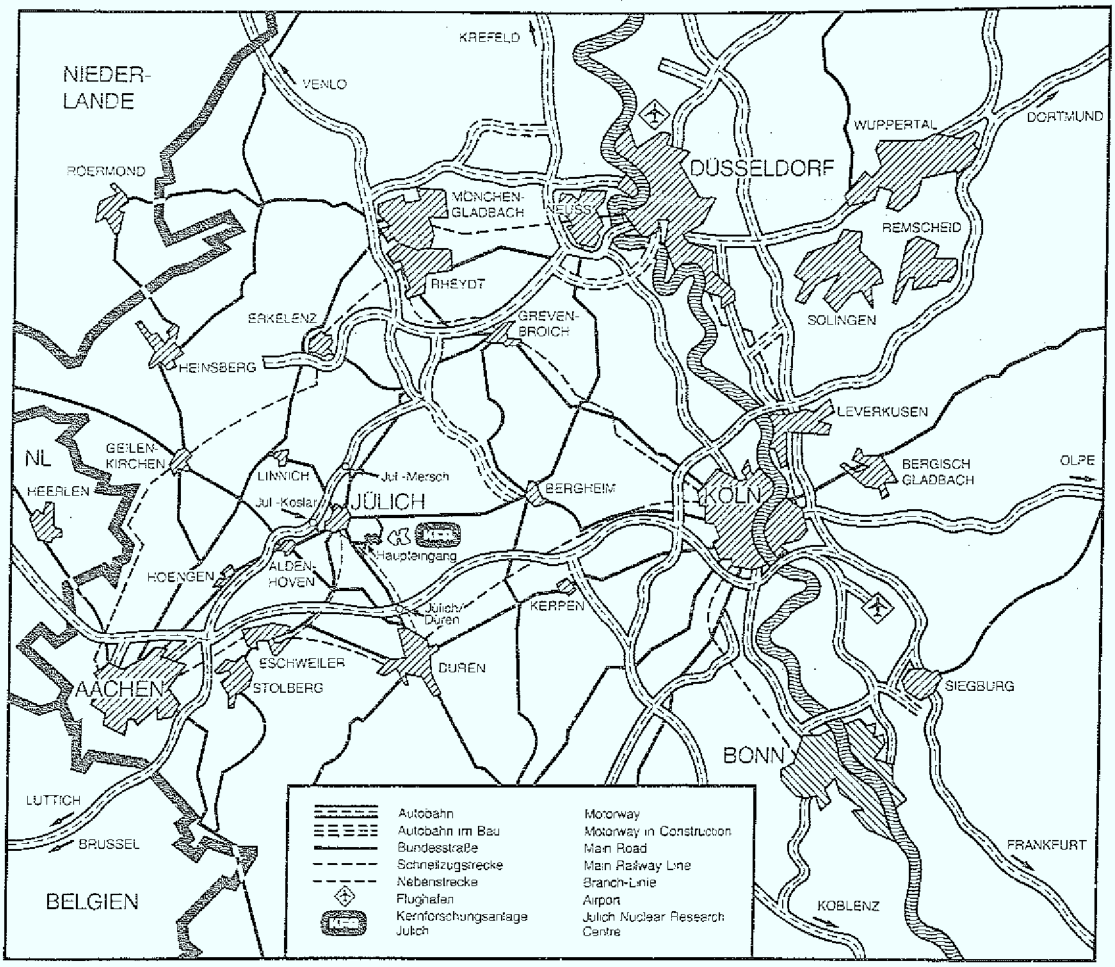

Als Manuskript gedruckt

Berichte der Kernforschungsanlage Jülich – Nr. 2116
Institut für Reaktorentwicklung Jül-2116

Zu beziehen durch: ZENTRALBIBLIOTHEK der Kernforschungsanlage Jülich GmbH
Postfach 1913 · D-5170 Jülich (Bundesrepublik Deutschland)
Telefon: 02461/610 · Telex: 833556-0 kf d

Reactor Physics Concept for a Low Enriched Compact Core

by

Hartwig Schaal
Istvan Vidovszky*

*Institute for Physics, Hungarian Academy of Sciences, Budapest

Reactor Physics Concept for a Low Enriched Compact Core

by

H. Schaal
I. Vidovszky*

*Institute for Physics, Hungarian Academy of Sciences, Budapest

Abstract

For a cylindrical compact core with fuel plates ordered in evolventic form and fueled with low enriched uranium, embedded in a D_2O tank, series of sensitivity studies were performed to achieve the criticality value k_{eff} as high as possible for fresh fuel core. Parameters studied are e.g. uranium amount, uranium enrichment, diameter of the core, cooling medium. The calculations were done using the Monte Carlo code MORSE in a modified version.

CONTENTS

1. Introduction

At KFA Jülich neutron scattering experiments are performed at the critical facility FRJ-2 (DIDO), which is a D_2O moderated and reflected reactor with a core consisting of 25 tubular fuel elements /1/. The maximum thermal fluxes of FRJ-2 lie at about 10^{14} $cm^{-2}s^{-1}$ /2/. Furthermore the ratio of thermal flux to fast and γ-flux is rather small. The facility began operation in 1962. So it is necessary to investigate possibilities to modernize the reactor. In the frame of these investigations a new core concept, which should give better thermal fluxes, is discussed /3/. This concept uses a cylindrical compact core with fuel plates of low enriched uranium fuel. Furthermore is demanded that the core can be operated at full power of 25 MW_{th} for a time period of at least 30 days.

This report investigates how such a core can be realized. To do this we performed a lot of sensitivity studies to find out how the reactivity value of the facility in the case of fresh fuel is affected by changes of diameter of the core, the uranium amount, coolant, the neutron radiation channels, the absorber elements, uranium enrichment, etc. Furthermore, burnup of the core is simulated to investigate the possible full power operation time, and finally we give the maximum thermal fluxes which can be achieved.

2. Core with D_2O coolant

Our first attempt to design a compact core inside the D_2O-tank consisted of a ring core with uranium plates which are cooled by D_2O. The active length of the uranium plates is 10 cm, the active height is 70 cm. A horizontal cross section of the core geometry is shown in fig. 1.

2.1 Generation of reaction cross sections

2.1.1 Problem dependent microscopic cross sections

For the generation of problem dependent group constants the two problem independent data libraries THERM-123 /4/ for the thermal data and, calculated by code SUPERTOG /5/, the socalled GGC-Library for the epithermal and the fast data were used. All data are based on ENDF/B-IV /6/.

To generate group cross sections in the fast and epithermal energy range, i.e. from 14.9 MeV to 0.41 eV, the code SPEKTRUS /7/ of the reactor calculation system RSYST /8/ was used. This code SPEKTRUS is able to calculate resonance cross sections for infinitely diluted resonance absorbers as well as for absorbers in plane, cylindrical, or spherical geometry. For our calculations with fuel plates the code was used in plane geometry. The important input parameters for the resonance calculation in SPEKTRUS are given in Table I. The procedure to calculate the Dancoff correction C is described in Appendix A. The result of the calculation are the problem dependent microscopic group cross sections σ_a, $\nu\sigma_f$, σ_{tot}, and $\sigma_{scatter}$ in 99 energy groups for temperature 323 K. It should be mentioned that these data do not contain upscattering.

For the thermal energy range, i.e. from 1.85 eV to 10^{-5} eV, starting point was the library THERM-123. This library contains moderator and all relevant fuel and absorber data in 123 energy groups.

Table I: Important input parameters for the resonance calculation

Nuclide density of ^{235}U	2.41×10^{21} cm^{-3}
Nuclide density of ^{238}U	9.77×10^{21} cm^{-3}
Nuclide density of ^{27}Al	3.04×10^{22} cm^{-3}
Nuclide density of Si	8.37×10^{21} cm^{-3}
Half thickness of meat	0.0275 cm
Dancoff correction	0.88

The group cross sections of the 99 group library were combined with the data of the 123 group library in the following manner: The elastic scattering from the fast and epithermal energy range into the thermal energy groups were calculated by code WQS /9/. The THERM-123 data were collapsed from 58 groups to 6 groups in the energy range from 1.85 eV to 0.41 eV using a spectrum which was got from a zero-dimensional spectrum calculation performed with code SPEKTRUM /10/. Then both libraries were combined. The result were microscopic group cross sections in 164 energy groups up to Legendre order P_1. The energy boundaries of the resulting library are given in Table II. We generated the 164 group library in the way described above because of three reasons:

a. We wanted to retain the energy group structure of the 99 group fast and epithermal library, because energy deposition coefficients of the library MACKLIB-IV /11/ are given in that energy structure.
b. We wanted to use data of the THERM-123 library in the energy range from 1.85 eV to 0.41 eV, because THERM-123 data contain upscattering.
c. For the lower thermal energy range we wanted to use the highest possible number of energy groups to get good energy resolution for the calculated spectra of the cold source which is foreseen to be run in the critical facility FRJ-2.

Table II: Energy group limits for 164 group library

Group No.	Upper Limit (eV)	Group No.	Upper Limit (eV)	Group No.	Upper Limit (eV)
1	1.4918E+07	56	2.4788E+04	111	3.0500E-01
2	1.3499E+07	57	1.9305E+04	112	2.9500E-01
3	1.2214E+07	58	1.5034E+04	113	2.8500E-01
4	1.1052E+07	59	1.1709E+04	114	2.7500E-01
5	1.0000E+07	60	9.1188E+03	115	2.6500E-01
6	9.0484E+06	61	7.1017E+03	116	2.5500E-01
7	8.1873E+06	62	5.5308E+03	117	2.4500E-01
8	7.4082E+06	63	4.3074E+03	118	2.3500E-01
9	6.7032E+06	64	3.3546E+03	119	2.2500E-01
10	6.0653E+06	65	2.6126E+03	120	2.1700E-01
11	5.4881E+06	66	2.0347E+03	121	2.0800E-01
12	4.9659E+06	67	1.5846E+03	122	2.0000E-01
13	4.4933E+06	68	1.2341E+03	123	1.9200E-01
14	4.0657E+06	69	9.6112E+02	124	1.8300E-01
15	3.6788E+06	70	7.4852E+02	125	1.7500E-01
16	3.3287E+06	71	5.8295E+02	126	1.6700E-01
17	3.0119E+06	72	4.5400E+02	127	1.5800E-01
18	2.7253E+06	73	3.5358E+02	128	1.5000E-01
19	2.4660E+06	74	2.7536E+02	129	1.4200E-01
20	2.2313E+06	75	2.1445E+02	130	1.3300E-01
21	2.0190E+06	76	1.6702E+02	131	1.2500E-01
22	1.8268E+06	77	1.3007E+02	132	1.1700E-01
23	1.6530E+06	78	1.0130E+02	133	1.0800E-01
24	1.4957E+06	79	7.8893E+01	134	1.0000E-01
25	1.3534E+06	80	6.1442E+01	135	9.5000E-02
26	1.2246E+06	81	4.7851E+01	136	9.0000E-02
27	1.1080E+06	82	3.7267E+01	137	8.5000E-02
28	1.0026E+06	83	2.9023E+01	138	8.0000E-02
29	9.0718E+05	84	2.2603E+01	139	7.5000E-02
30	8.2085E+05	85	1.7603E+01	140	7.2000E-02
31	7.4274E+05	86	1.3710E+01	141	6.8000E-02
32	6.7206E+05	87	1.0677E+01	142	6.4000E-02
33	6.0810E+05	88	8.3153E+00	143	6.0000E-02
34	5.5023E+05	89	6.4760E+00	144	5.6000E-02
35	4.9787E+05	90	5.0435E+00	145	5.2000E-02
36	4.5049E+05	91	3.9279E+00	146	4.8000E-02
37	4.0762E+05	92	3.0590E+00	147	4.4000E-02
38	3.6883E+05	93	2.3824E+00	148	4.0000E-02
39	3.3373E+05	94	1.8554E+00	149	3.7000E-02
40	3.0197E+05	95	1.4400E+00	150	3.4000E-02
41	2.7324E+05	96	1.1250E+00	151	3.1000E-02
42	2.4724E+05	97	8.7600E-01	152	2.8000E-02
43	2.2371E+05	98	6.8200E-01	153	2.0000E-02
44	2.0242E+05	99	5.3100E-01	154	2.2500E-02
45	1.8316E+05	100	4.1300E-01	155	2.0000E-02
46	1.6573E+05	101	4.0000E-01	156	1.7500E-02
47	1.4996E+05	102	3.9000E-01	157	1.2000E-02
48	1.3569E+05	103	3.8000E-01	158	1.3000E-02
49	1.2277E+05	104	3.7500E-01	159	1.1000E-02
50	1.1109E+05	105	3.6500E-00	160	9.0000E-03
51	8.6517E+04	106	3.5500E-01	161	7.0000E-03
52	6.7379E+04	107	3.4500E-01	162	5.0000E-03
53	5.2475E+04	108	3.3500E-01	163	3.0000E-03
54	4.0868E+04	109	3.2500E-01	164	1.0000E-03
55	3.1828E+04	110	3.1500E-01		

Lowest energy of the library is 1.0000E-5 eV

2.1.2 Homogenized macroscopic cross sections for the core region

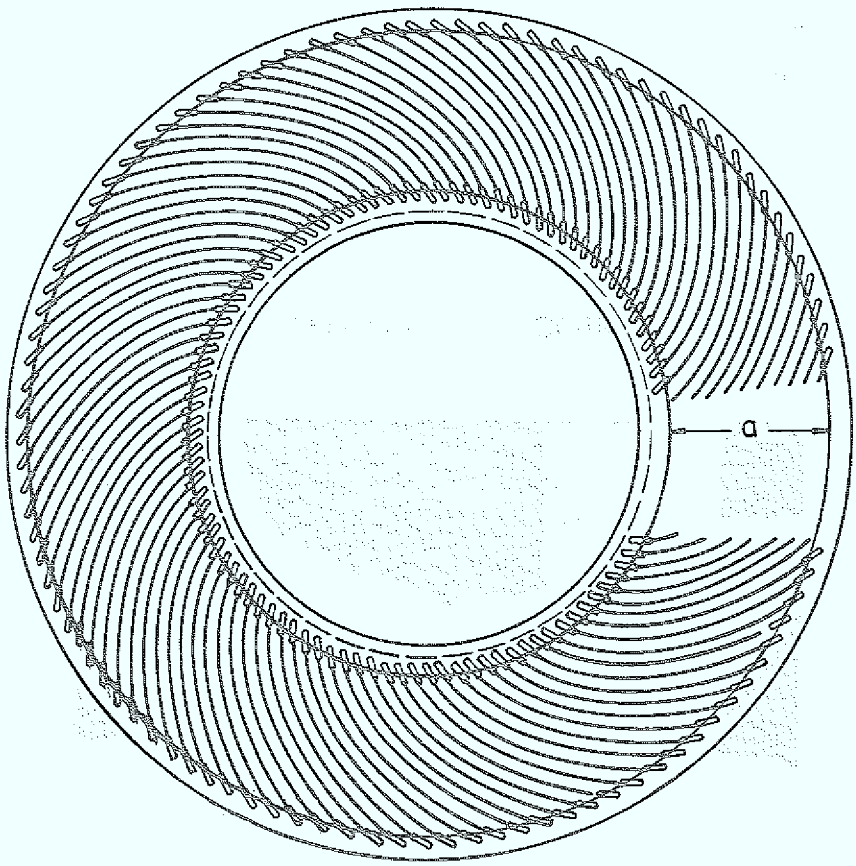

Fig. 1: Horizontal cross section of the compact core with fuel plates ordered in evolventic form

Because it is very difficult for the Monte Carlo calculations to take into account the complex geometry of the fuel plates, which are ordered in evolventic form (see fig. 1), and of the cooling gaps, this region was treated as homogeneous. To get the homogenized cross sections for this region consisting of meat, cladding, and D_2O-cooling gap between the fuel plates, a one-dimensional cell calculation with code ISOSTO /12/ was performed for plane geometry (see fig. 2). We chose white boundary conditions for the cell calculations, i.e. we considered an infinite number of fuel plates and gaps. Input parameters for the calculation are given in Table III. The result of the calculation are zone dependent neutron fluxes for 164 energy groups. These fluxes are used by code MITHOM of the code system RSYST to homogenize the cross sections of the zones. So the homogenized macroscopic cross sections for the core region take into account the flux disadvantage factors of the heterogeneous structure.

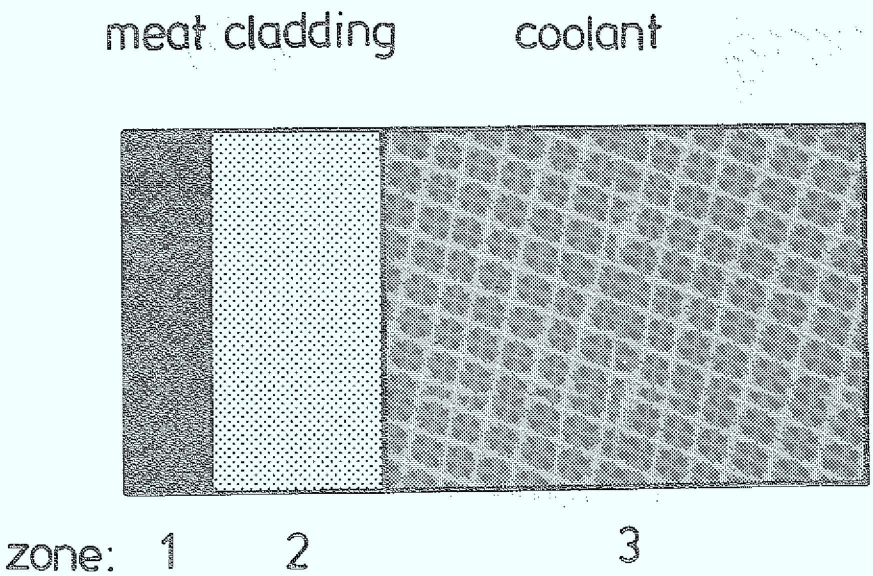

Fig. 2: Unit cell for ISOSTO calculation

Table III: Important input parameters for the cell calculation

Zone	Thickness (cm)	Material	Number Density (10^{24} cm^{-3})
meat	0.0275	^{235}U	2.41×10^{-3}
		^{238}U	9.77×10^{-3}
		^{27}Al	3.04×10^{-2}
		Si	8.37×10^{-3}
cladding	0.033	^{27}Al	6.00×10^{-2}
cooling gap	0.1	D_2O	3.00×10^{-2}

2.2 Calculation of k_{eff}-values for simple geometry

The criticality calculations for the entire facility were performed using the Monte Carlo code MORSE /13/ in a version modified by IRE/KFA and running on CRAY-XMP. The geometry used in the MORSE calculations is shown in figs. 3 and 4. In radial direction one can see in the center the region 1 filled with D_2O. It follows region 2 which is the inner aluminum ring with thickness 1 cm. Region 3 is the core region with homogenized cross sections, region 4 is the outer aluminum ring with thickness 1.1 cm, and region 5 is the D_2O-tank with outer radius 125 cm. In axial direction one can see the core region with height 70 cm, then two aluminum rings of height 15 cm each, and finally the D_2O-tank with height 250 cm. This simple geometry was used to perform sensitivity studies for different core radii, different cooling gap thicknesses, and different uranium densities in the meat of the fuel plates.

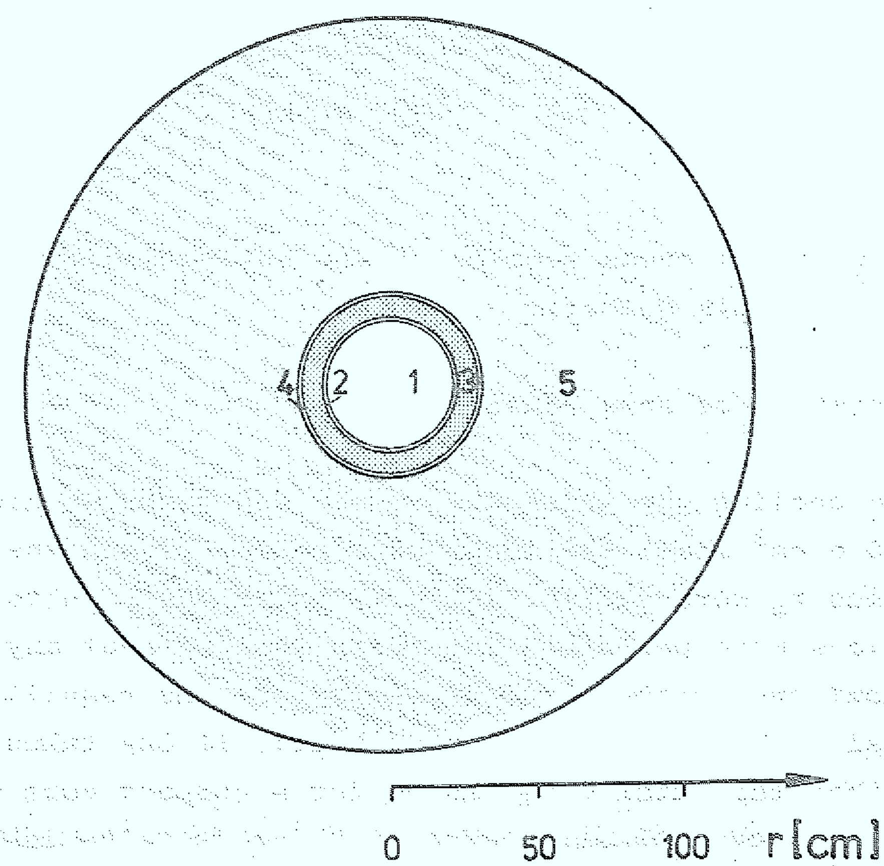

Fig. 3: Horizontal cross section of the entire facility in case of simple geometry

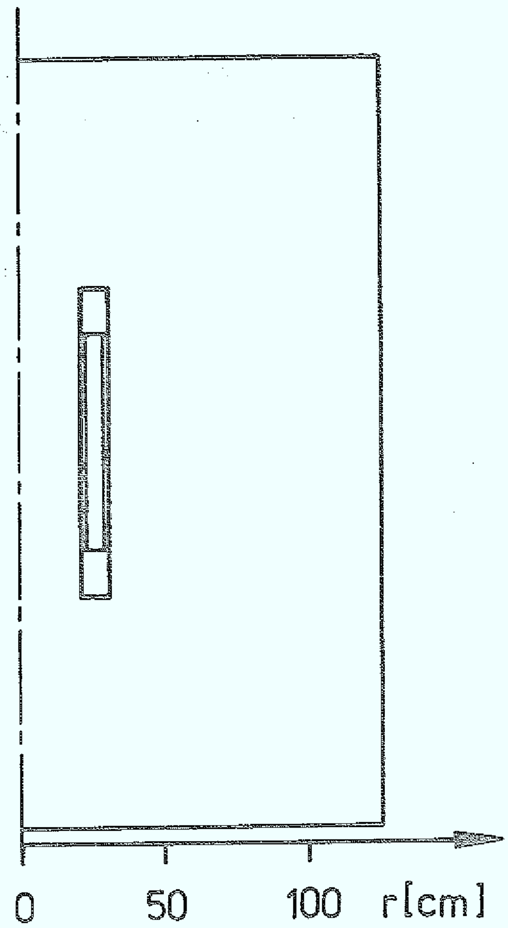

Fig. 4: Vertical cross section of the entire facility in case of simple geometry

2.2.1 Variation of core radii

For fixed cooling gap thickness (2 mm) and fixed uranium density (4.8 g/cm^3 meat) the inner core radius r_i and the outer core radius r_a were varied. Table IV shows the results. The calculations were performed for fresh fuel without any burnup and without any poisoning of Xe and Sm. So the resulting criticality values k_{eff} seem to be very small. If one takes into account that the outer core radius for a compact core should not be larger than 20 cm because of the flux value inside the D_2O-reflector, it is clearly shown that the core configurations considered here are worthless.

Table IV: Variation of core radii in case of D_2O coolant

Core radius inner r_i(cm)	outer r_a (cm)	^{235}U-amount (kg)	k_{eff}
7.06	14.3	5.3	0.976
12.2	19.3	7.96	1.076
22.8	30.0	13.37	1.151

2.2.2 Variation of cooling gap thickness

To get larger k_{eff} values, we changed the cooling gap thickness from 2 mm to 2.2 mm. The cell calculation (see section 2.1.2) with the new gap thickness of 2.2 mm gave the value k_∞=1.356, which is not far from the value k_∞=1.336 for the gap thickness of 2 mm. So it is not worth while to perform a MORSE calculation for the larger gap thickness.

2.2.3 Variation of uranium density

The uranium density in the meat was enlarged from 4.8 g/cm^3 to 6.5 g/cm^3. The cell calculation with data of higher uranium density gave k_∞=1.336 for density 4.8 g/cm^3. So it is shown that with higher uranium density the facility is not able to reach higher k_{eff} values.

3. Core with H_2O coolant

The results of section 2 have shown that it is not possible to get compact cores with 19.75 percent uranium enrichment which are cooled by D_2O. So we investigated cores which have got the same uranium enrichment, i.e. 19.75 percent, but which use H_2O coolant.

3.1 Generation of reaction cross sections

The cross sections needed for the calculation of an H_2O cooled core were generated in the same way as described in section 2.1. For the generation of the resonance cross sections the Dancoff correction for a 2 mm thick cooling gap filled with H_2O is C=0.58 because of $\sigma_{epi}(H_2O)$=44 barns. The cell calculation for the unit cell consisting of meat, cladding, and H_2O cooling gap leads to k_∞=1.665 which is much higher than in the case of D_2O cooling.

3.2 Calculation of k_{eff}-values for simple geometry

With the generated problem dependent cross sections in 164 energy groups we performed criticality calculations for the same configurations as we had done for cores with D_2O coolant.

3.2.1 Variation of core radii

We treated three cases of core radii. In the first case the outer radius r_a is much smaller than 20 cm, in the third case it is much larger. The results of the calculations are shown in Table V. It can be stated that the first case (r_a=12.7 cm) has got a value k_{eff} which is too low. The second case leads to a reasonable high k_{eff}. The third case shows that the increase of r_a gives some increase in k_{eff}, but this case is of no interest because the increase in radius leads to decreasing fluxes in the D_2O-tank.

Table V: Variation of core radii in case of H_2O coolant

Core radius inner r_i(cm)	Core radius outer r_a (cm)	^{235}U-amount (kg)	k_{eff}
7.06	12.7	3.92	1.112
12.2	19.3	7.96	1.267
22.8	30.0	13.37	1.309

3.2.2 Axial partitioning of the core region

It was considered to construct a compact core of two parts which could reach higher burnup by changing lower and upper part after a given time of full power operation. Furthermore an axial partitioned core could give much better neutron beam quality for beam tubes in radial direction, because these tubes would not point into the direction of fuel and therefore would avoid a direct line of sight from fuel to the experiments for the fast neutrons and the γ-flux.

For the geometry of the calculational procedure the axial partitioning means that the core region in devided into two axial parts of height 30 cm each, with a gap of 10 cm height filled with H_2O coolant. The geometry is shown in fig. 5. In that figure one can see six rings around the core inside the D_2O-tank. These are volume detector zones to calculate the neutron flux distribution. The flux values are of interest to answer the questions, which maximum thermal flux can be achieved and at which distance from core center this maximum flux is found.

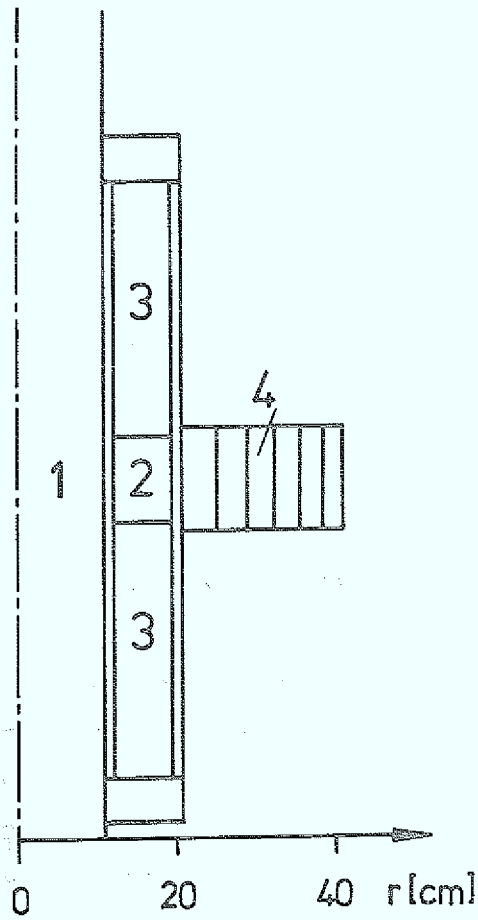

Fig. 5: Vertical cross section of partitioned core
(1 = central channel, 2 = gap between half cores,
3 = core regions, 4 = volume detector regions inside
D_2O tank)

We shall compare the results of two calculations with H_2O in the center (region 1 of fig. 3), one of these calculations performed without the H_2O gap (i.e. with core height 70 cm), the other one performed for the axial partitioned core described above. The results are given in Table VI and in fig. 6. One can see that the partitioning of the core leads to much smaller k_{eff} but to higher thermal fluxes.

Table VI: Influence of axial partitioning of the core with H_2O in the central channel

Arrangement of the core	^{235}U-amount (kg)	k_{eff}
not partitioned, i.e. 70 cm high	7.96	1.100
axial partitioned, i.e. 2x30cm core region+10cm H_2O gap	6.81	0.963

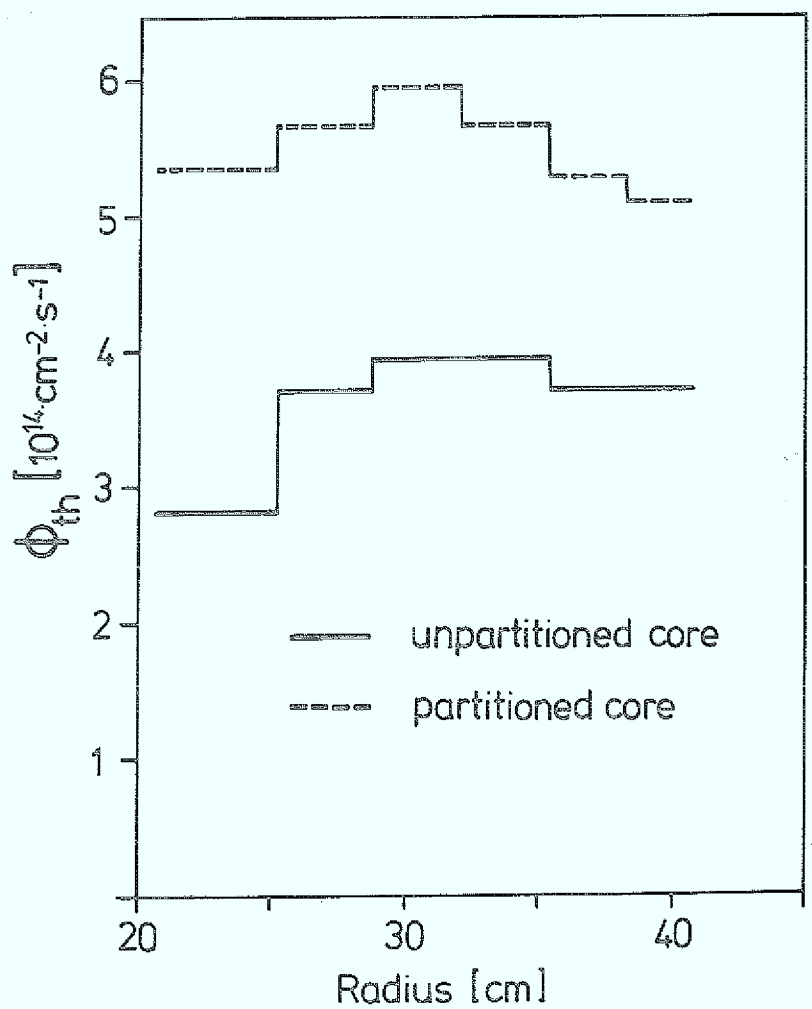

Fig. 6: Radial distribution of thermal neutron flux ($E_n \leq 0.41$ eV) inside D_2O tank for partitioned and unpartitioned core with H_2O fluid in central channel (reactor power is 25 MW)

3.2.3 Reflecting material in the central channel

We have seen in section 3.2.2 that the advantages of better beam quality and higher burnup given by the partitioned core cannot be reached with water in the central channel. So we now put in an inner reflector, i.e. a beryllium rod removes the water (region 1 of fig. 5) to increase the k_{eff}-value. The comparison of this case with that containing H_2O in the central channel is given in Table VII and in fig. 7. It can be seen that for the case with the beryllium reflector in the middle k_{eff} reaches reasonable amount. On the other hand the neutron flux maximum is by about 17 percent smaller than in the case of H_2O channel material. To make the configuration more realistic we changed the material of the 10 cm high gap from H_2O to the real structure, i.e. to 38 volume percent aluminum and 62 volume percent water. The beryllium rod remained in the central channel. So we got k_{eff}=1.158. Then we introduced a cooling channel of 1 cm thickness between the rod and the inner aluminum ring of the core. The resulting value then is k_{eff}=1.138.

Table VII: Variation of material in the central channel for axial partitioned core

Material in central channel	k_{eff}
H_2O	0.963
Be	1.136

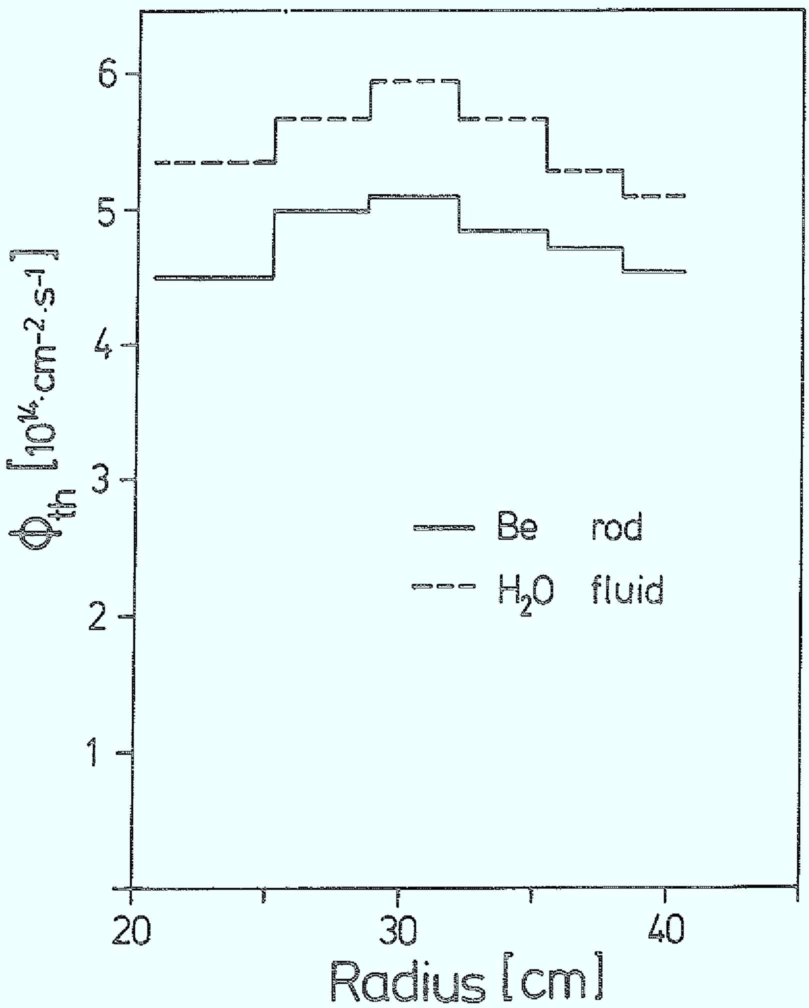

Fig. 7: Radial distribution of thermal neutron flux ($E_n \leq 0.41$ eV) inside D_2O tank for partitioned core with H_2O fluid or beryllium rod in central channel (reactor power is 25 MW)

3.2.4 Higher uranium density

Next step to reach a criticality value k_{eff} as high as possible for the axial partitioned core with 19.75 percent enriched uranium fuel was the increase of the uranium density in the meat from 4.8 g/cm^3 to the maximum possible value of 6.5 g/cm^3. This increase in density leads to an increase of the amount of ^{235}U from 6.81 kg to 9.22 kg. The achieved criticality value is then k_{eff}=1.174. The thermal neutron flux distribution in the D_2O-tank around the core is shown in fig. 8.

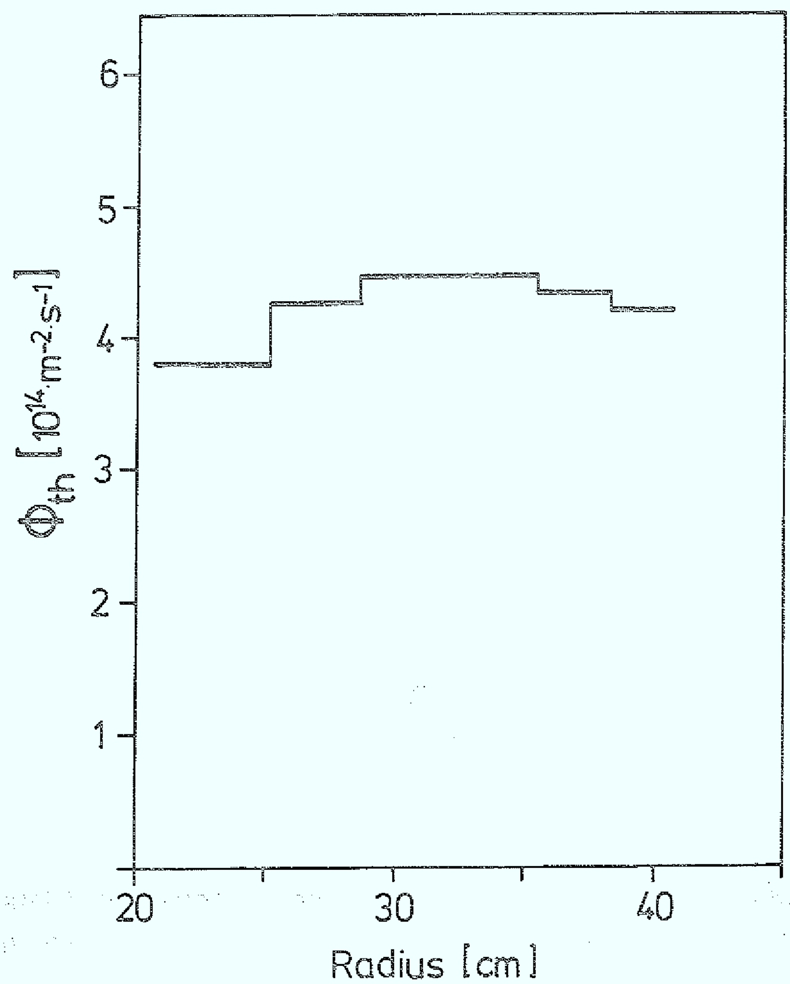

Fig. 8: Radial distribution of thermal neutron flux (E_n≤0.41 eV) inside D_2O tank for partitioned core with beryllium rod in central channel and uranium density 6.5 g/cm^3 meat (reactor power is 25 MW)

3.2.5 Simulation of burnup

We wanted to answer the question how k_{eff} will change for different burnup levels of the 19.75 percent enriched fuel. To avoid the burnup calculations, which are very time consuming, we simulated the burnup levels by reducing the amount of ^{235}U to take into account the loss of fuel and by adding boron to take into account the absorption caused by the fission products. It was assumed that each fission leads to an absorption cross section of the fission products of 80 barns /14/. This leads to the following numbers: For burnup of 1000 MWd one gets the decrease of ^{235}U of 1.05 kg and the increase of ^{10}B of 0.93 g because of the ^{10}B-thermal absorption cross section of 3837 barns /15/.

The burn up calculations were performed for cases of one core region and for cases where the core region was devided into different radial zones with different burn up levels proportional to the neutron flux values of the fresh fuel core zones. Furthermore MORSE calculations with identical input but different starting random numbers were performed. The result of all these calculations is shown in fig. 9. It can be seen that the decrease of k_{eff} is nearly 5 percent per 1000 MWd, i.e. per 40 days of full power operation.

3.3 Realistic geometry

As it was shown in section 3.2 the water cooled and D_2O reflected configuration gives a sufficient value of k_{eff} if the geometry is simplified, i.e. the details of the real reactor outside the core are neglected. The next step of the investigations should take into account these details too.

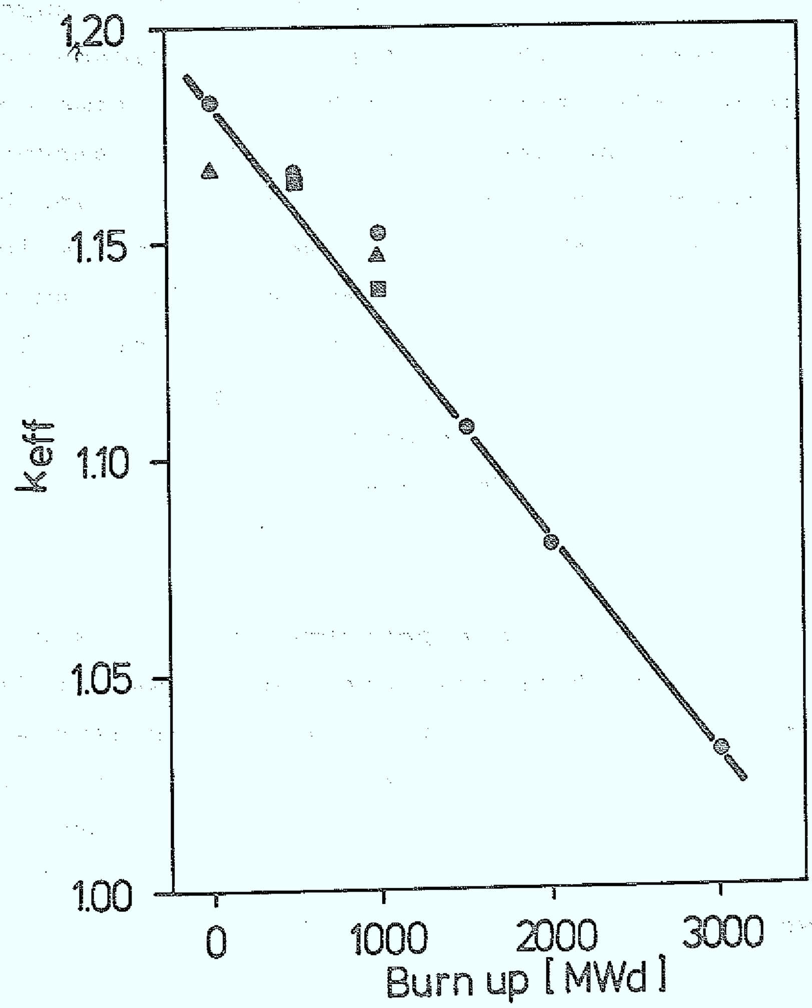

Fig. 9: Dependence of k_{eff} on burn up level
(▩ = one core region only, ● = two radial core regions, calculation with some stating random number, ▲ = two radial core regions, calculations with different starting random number)

The realistic geometry of the reactor was designed according to the plans described in /3/. It is shown in figures 10, 11, and 12. In fig. 10 one can see the horizontal cross section of the facility in the middle of the reactor height. In the center (regions 1 to 4) we find the same situation as for the simple geometry. But then the situation changes. The core is surrounded by two guide tubes of aluminum of 1 cm thickness. Between the tubes we find a gap of 1 cm thickness. These tubes separate the H_2O area from the D_2O tank. The area of the tubes and the gap is denoted as region 5 in fig. 10. Inside the D_2O tank one can see a lot of irradiation channels. The walls of the channels are made of aluminum with thickness 1 cm. The inner diameters of the tubes are 10, 6 or 4 inches, respectively. The dashed lines show 2 tubes which lie 30 cm below the middle plane of the reactor. In vertical direction 3 channels are found. The largest one is foreseen to contain the cold source.

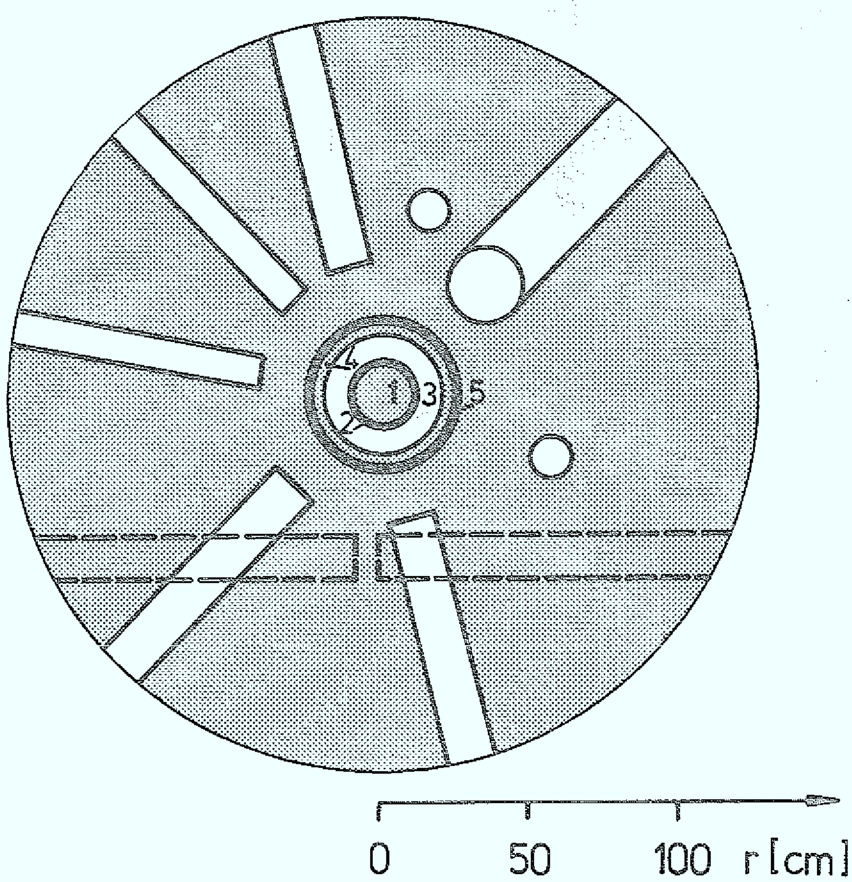

Fig. 10: Horizontal cross section of entire facility with neutron beam tubes

Fig. 11 gives a vertical cut of the assembly. In the center of the facility one finds a beryllium rod which serves as inner reflector. Below and above the core the regions are filled with the cooling water. The vertical tube which ends inside the D_2O-tank is the tube for the cold source.

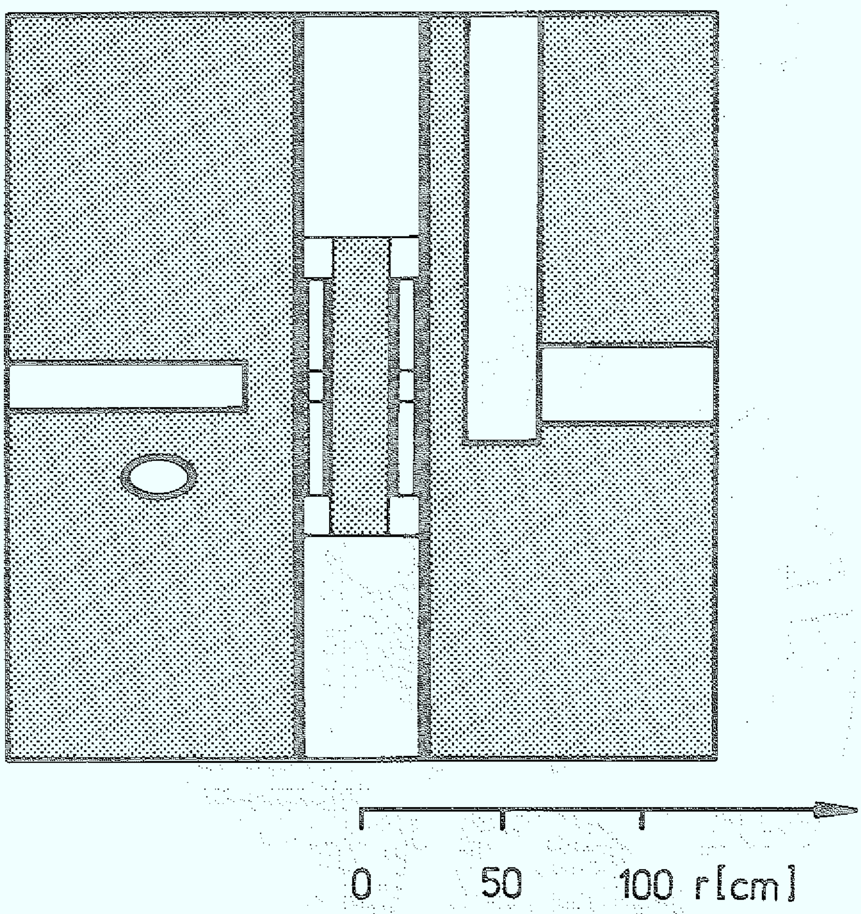

Fig. 11: Vertical cross section of entire facility with neutron beam tubes

Fig. 12 shows in detail the area of core region and guide tubes. The space between the two guide tubes is filled with H_2O to cool the absorbers which are foreseen to be moved in this gap.

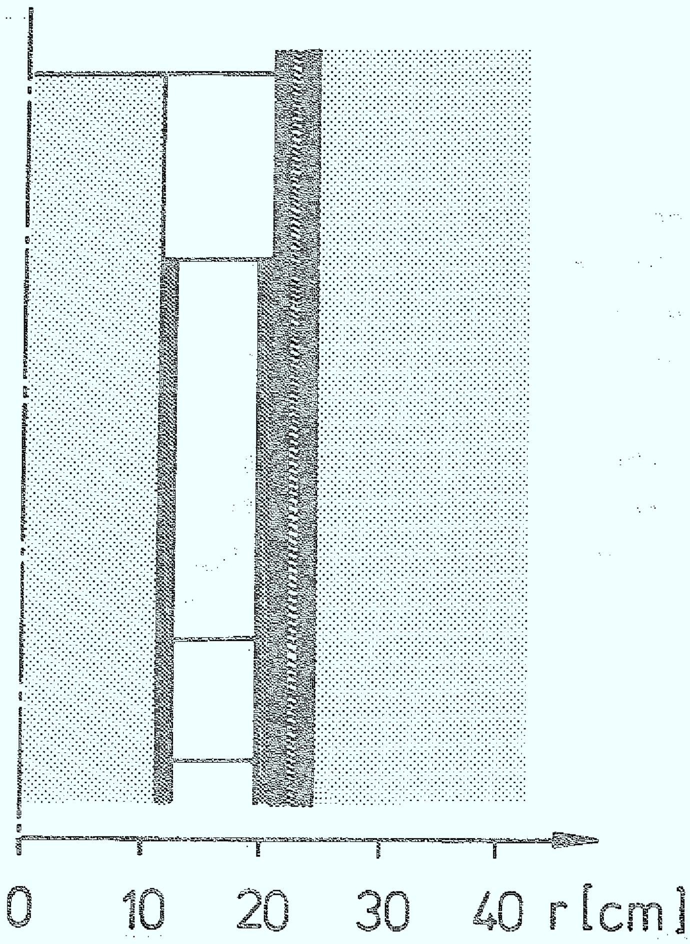

Fig. 12: Detail of vertical cross section to show the core tubes (dark areas) around the core region

The MORSE calculations resulted in k_{eff}=1.063 for this case. If we compare this value to the k_{eff}=1.17 of the simplified geometry, we find the difference rather great. To clear up, which part of the reactor is responsible for this big effect, detailed studies have been carried out, as described in 3.3.1 and 3.3.2. Before going into details, we have to make the decisive statement, that the low k_{eff} value of the initial state of the reactor (fresh fuel etc.) does not allow to utilize a reactor according to the geometry, shown in figures 10, 11, and 12.

3.3.1 Influence of irradiation channels

To check the influence of irradiation channels the following series of calculations has been carried out by MORSE for the cases:

- completely realistic arrangement
- irradiation channels filled with D_2O
- channel walls filled with D_2O too
  (i.e. there are no irradiation channels).

The results of these calculations are summarized in Table VIII. As one can see in Table VIII, the differences are rather small, i.e. the significant factor reducing k_{eff} is not the influence of the irradiation channels, but the influence of structures, placed near to the core. Therefore, in the next subsection the influence of these elements is analyzed.

Table VIII: Influence of the irradiation channels

No.	Configuration	k_{eff}
1	Real geometry	1.063±0.014
2	D_2O inside the irradiation channels	1.059±0.010
3	Channel walls filled by D_2O too (i.e. channels exist only in geometry description, but not in reality)	1.077±0.009
4*	No irradiation channels at all (i.e. irradiation channels removed fom the geometry description too)	1.068±0.012

*This case was calculated only to test the correctness of geometry description. Cases 3 and 4 are identical from the first point of view of physics. The agreement between k_{eff} for these cases is satisfactory (with the limit of the errors).

So we can conclude, that the geometry shown in figures 10, 11, and 12 does not allow to make feasible the reactor, but if we reduce the amount of absorbing material in that region, a sufficient value of k_{eff} can be reached, even if irradiation channels are taken into account.

The two parallel tubes have been foreseen to hold the control rods. The control rods were foreseen to move inside the water gap between the two tubes. If we consider control rods inside the core (i.e. between core and Be reflector), or control rods outside the core, but moved in D_2O, than one tube is sufficient, as it has the only aim to separate water (coolant) from D_2O (reflector). Calculations have been carried out, considering only one aluminum tube (and consequently no water gap) of two different thicknesses. The results are given in Table X.

Table X: Variation of core tube thickness

Tube thickness (cm)	k_{eff}
1.0	1.116
0.7	1.129

These results show, that the k_{eff} values are very close to the minimum acceptable values, even if one takes into account the errors, it is not quite sure, whether they are acceptable at all (considering Xe and Sm poisoning and 1000 MWd burnup).

3.3.3 Varying of the D_2O tank radii

As it can be seen in figures 10 and 11 the whole reactor core is situated in a tank, filled with D_2O. The sizes of this tank are defined according to technical aspects. To be sure, that any radius of technical interest is possible without limiting

3.4.1 Absorber cross sections

The data for the absorber materials were generated in a similar fashion as described in section 2.1. The only difference was that the 99 energy group data for the fast and epithermal energy groups were combined with the lower 65 energy groups of the data library THERM-123. This was done because the thermal data for the absorber materials did only contain absorption cross sections but not scattering data. For hafnium no thermal data were available. Therefore we introduced the absorption cross section data of ^{10}B, but with the dilution factor f=0.028 to get the correct thermal cross section of σ_a=105 barn at 2200 m/s velocity. This σ_a-value for hafnium is taken from /16/.

3.4.2 Absorber configurations

As a first step of absorber studies the isotope ^{10}B as absorber was concerned. The aim of these studies was to show the influence of absorber elements on k_{eff} in different positions, to find out the most sufficient absorber configurations.

The possible positions of absorber elements are designed according to the technical project of the reactor. There are two main possibilities: inside the core (i.e. between fuel and Be reflector) or outside the core (i.e. between fuel and D_2O reflector). In both cases the absorbers have the shape of rings, the upper one 70 cm long, the lower one 30 cm long. The upper ring inside is divided into three, the upper ring outside into four parts, all parts having identical shape and volume and placed symmetrically in case of normal operation of the reactor. Normally, the upper ring can be moved downwards until the middle of the core, while the lower part can be moved upwards until the core middle as well. In case of emergence shut down the upper absorbers can fall down to the lower edge of the core region. The k_{eff} values for different absorber positions have been calculated by means of the code MORSE as well. The results for absorber elements outside the core are given in Table XII, while for absorber elements inside in Table XIII.

Table XII: Influence of absorber elements which are placed outside the core

No.	Arrangement	k_{eff}
1	No absorbers in the system (reference)	1.112 ±0.0094
2	All absorbers are at their endpositions (out of core)	1.084 ±0.0042
3	One absorber element (a quarter of the ring) is in the core (throughout) all other absorbers at their endpositions	1.009 ±0.0086
4	Two absorber elements are inside, all others are at their endpositions	0.932 ±0.0140

The results show, that the absorber elements, when pulled out (into their endpositions) have a non-negligible influence on the k_{eff} value in both cases (No 2 in Tables XII and XIII).

Table XIII: Influence of absorber elements which are placed in the central channel

No.	Arrangement	k_{eff}
1	No absorbers in the system (reference)	1.119±0.007
2	All absorbers are at their endpositions (out of core)	1.105±0.014
3	One absorber element (a third of the ring) is in the core (throughout) all other absorbers at their endpositions	0.998±0.009

This influence inside the core is somewhat smaller than outside, but if one considers the given statistical errors, this difference is not significant. On the other hand one can see from the tables, that one absorber element is insufficient to shut down the core with acceptable safety (k_{eff} should be less than 0.95) inside as well as outside. On the basis of these results one has to consider other absorber media than ^{10}B. As the comparison of the results shows, that the position inside the core is more advantageous than outside, the different materials have been tested only inside the core. The detailed description of these studies follows in 3.4.3.

3.4.3 Different absorber materials

An optimum absorber should have minimum influence at the end-position (out of core) and a maximum influence at the working position (in the core). A rough estimation of the neutron fluxes in these two positions (in the core - out of the core) gives, that the relations of flux in the core to flux outside the core are for the

- fast energy range (i.e. 14.9 MeV - 1 MeV) 20:1
- epithermal energy range (i.e. 1 MeV - 0.41 eV) 10:1
- thermal energy range (i.e. 0.41 eV - 10^{-5} eV) 2:1.

On the basis of that one can presume, that the optimum absorber should have significant absorbing cross sections at higher energies. Two absorbers have been considered, the first one a silver-indium-cadmium alloy, consisting of 80-15-5 weight%, respectively, while pure hafnium metal as the second one.

Table XIV: Influence of different absorber materials for absorber elements placed in the central channel

Position / Material	All absorber elements at their endpositions (out of core)	One absorber element (one third of a ring) in the core
Boron	1.091±0.008	0.993±0.010
Silver-indium-cadmium alloy (80-15-5)	1.109±0.007	0.997±0.007
Hafnium (metal)	1.096±0.004	1.022±0.007

The densities are 9.53 g/cm^3 for the alloy and 13.31 g/cm^3 for hafnium according to data from /17/. The k_{eff} calculations for the different materials have been carried out by means of the code MORSE. The results are listed in Table XIV, for the convenience of the comparison results for ^{10}B absorber are given here as well. The results in the table show, that there is no significant difference between these three types of absorber material. Even the thermal absorber boron is somewhat more effective than the other two epithermal absorbers. This effect is easy to understand if one looks to figure 13, where the macroscopic cross sections are plotted versus energy. The macroscopic cross section of boron absorber is higher within the whole energy range, than that of the other two absorbers. We conclude that all absorbers are equivalent.

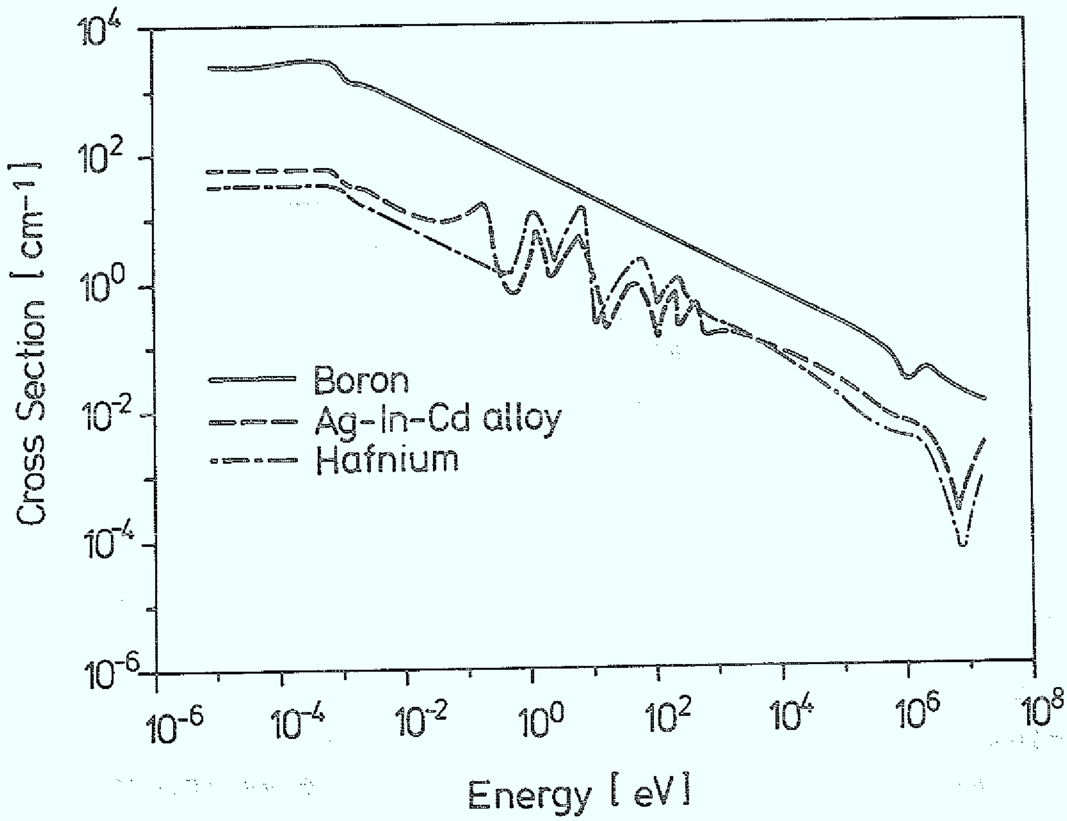

Fig. 13: Macroscopic cross sections of different absorber materials

3.5 Sensitivity of axial partitioning

All calculations performed for the axial partitioned core had used an axial partitioning zone of 10 cm height consisting of 62 volume-percent H_2O and 38 volume-percent Al. The results have shown that for the maximum case, i.e. uranium density in meat 6.5 g/cm^3 and Hf-absorbers in endposition, the highest k_{eff}-value was k_{eff}=1.11, which seems to be insufficient for fresh fuel cores. So we tried to reduce the height of the partitioning zone to find out how strong the increase of k_{eff} would be. Table XV shows the result. The case of 0 cm height means that the core is not partitioned. It can be seen that for the height 5 cm, which is technically feasible, one gets reasonable high k_{eff} for fuel with ^{235}U-enrichment of 20 percent. But it should be mentioned that the decreasing height of the partitioning zone leads to a decreasing beam quality as was described already in section 3.2.2.

Table XV: Variation of axial partitioning zone height

Height of axial partitioning zone (cm)	Amount of ^{235}U (kg)	k_{eff}
10	9.22	1.110
7	9.68	1.137
5	9.99	1.156
0 (unpartitioned)	10.76	1.193

3.6 Different uranium enrichment

Besides the possibility to enlarge k_{eff} by reducing the partitioning zone it should be possible to increase the uranium enrichment. All calculations until now were performed for ^{235}U-enrichment of 19.75 percent.

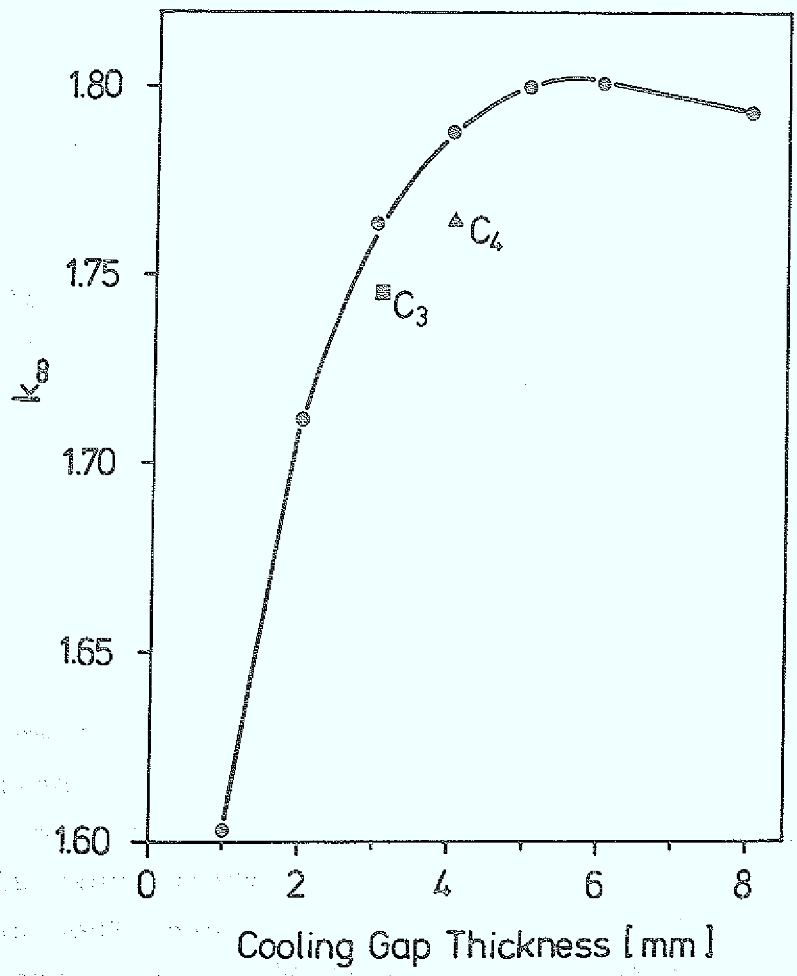

Fig. 14: Dependence of k_∞ on cooling gap thickness (C3, C4 = calculations performed with adequate resonance data)

The figure shows that k_∞ is increasing up to a gap thickness of 6 mm. But it should be mentioned that the resonance cross sections for this sensitivity study were taken from the case of 2 mm gap thickness. Therefore, we calculated the resonance data for 3 mm and 4 mm gap thickness and so we got the correct k_∞ values, denoted as C3 and C4 in fig. 14. With these correct data the MORSE calculations were performed for the different cases of gap thickness. The result of the calculations is shown in Table XVII. It can be stated that the increase in k_∞ for increasing gap thickness does not lead to increasing k_{eff}.

Table XVII: Influence of cooling gap thickness in case of 40 per cent enriched uranium fuel

Cooling gap thickness (cm)	^{235}U-amount (kg)	Resonance integral (barns) ^{235}U	^{238}U	k_∞	k_{eff}
2	18.44	194.6	50.6	1.711	1.152
3	14.06	204.8	59.7	1.745	1.159
4	11.36	210.0	65.4	1.764	1.155

3.6.3 Power distribution inside the core

For the case of 40 percent uranium enrichment with 2 mm cooling gap thickness we calculated the power distribution inside the core for the following case: fresh fuel without any Xe- or Sm-poisoning. The Hf-absorber rings have got their inner edges 12 cm above and below the middle plane of the core. Then criticality value k_{eff}=1.007 is achieved. Both half cores were devided into 7 radial and 10 axial zones of different thicknesses (see fig. 15). Symmetrical zones of upper and lower half core were treated as identical to get minor statistical uncertainties for the calculation of the power density distribution. The total power of the facility is assumed to be the maximum power, i.e. 25 MW. The mean value of the power density is about 0.6 kW/cm^3. Fig. 15 shows the calculated power distribution. One can see that the absorber rings push, as expected, the power densities in radial direction to the outer edge of the core and in axial direction to the inner edges of the half cores.

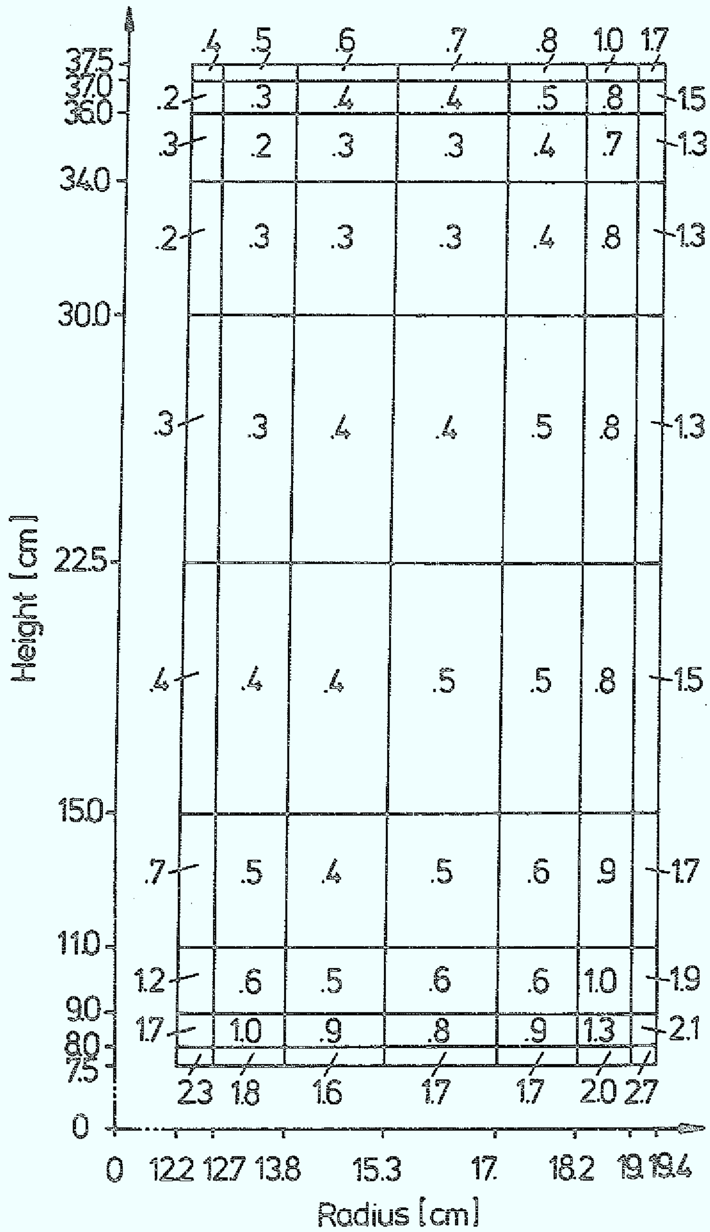

Fig. 15: Power density distribution inside core of fresh fuel with k_{eff} = 1.007 (power density values plotted in kW/cm^3); reactor power is 25 MW)

4. Conclusion

We want to answer the question, which core concept would be the feasible one. To do this we first look at the calculated k_{eff}-value that is necessary for the fresh fuel core with absorbers in endpositions. This value has to be at least $k_{eff} = 1.13$ because of the following facts:

- Xe- and Sm-poisoning give rise to $\Delta k/k \sim 4$ percent,
- temperature increase above 50°C may give rise to $\Delta k/k$ upto 1 percent,
- burnup of 1000 MWd feeds to $\Delta k/k \sim 5$ percent,
- statistical uncertainties of the calculations lie within the region of $\Delta k/k \sim 2$ percent,
- contingencies may lead to $\Delta k/k \sim 1$ percent.

Second we demand good neutron beam quality for beam tubes in radial direction. Therefore the axial partitioned core with 15 cm high gap is to be preferred.

These demands lead to the concept of the compact ring core with about 40 percent enriched uranium fuel.

5. References

/1/ Sicherheitsbericht für den Betrieb des Forschungsreaktors FRJ-2 (DIDO) vom 1. Februar 1962 mit Ergänzung vom Oktober 1970
vorgelegt von der KFA Jülich GmbH

/2/ G. Bauer, KFA-internal report MJF000004.01, 28.10.1985

/3/ J. Nöcken, G. Thamm
KFA-internal report MJF000013.01, 29.1.1986

/4/ THERM-123
Eine Datenbibliothek für thermische Neutronenwirkungsquerschnitte
IKE Bericht-Nr. 6-61/1 und 6-61/2, Januar 1973

/5/ R.Q. Wright, N.M. Greene, J.L. Lucius, C.W. Craven, Jr.
SUPERTOG: A Program to Generate Fine Group Constants adn P_n Scattering Matrices from ENDF/B
ORNL-TM-2679, September 1969

/6/ D. Garber, C. Dunford, S. Pearlstein
ENDF-102. Data Formats and Procedures for the Evaluated Nuclear Data File, ENDF
BNL-NCS-50496, October 1975

/7/ GGC-4. Multigroup Cross Section Code
CCC-GA-9021

/8/ R. Rühle: RSYST: Ein integriertes Modulsystem mit Datenbasis zur automatischen Berechnung von Kernreaktoren
IKE Bericht-Nr. 4-12, Juli 1973

/9/ H. Wohland
Streumomente bei isotroper Streuung im Schwerpunktsystem mit 1/E-Flußwichtung und ruhendem Zielkern
IKE Bericht-Nr. 4-4 3-3.10.1170, Januar 1972

/10/ R. Rühle: SPEKTRUM
IKE Bericht-Nr. 3-3.5.1096 (1970)

/11/ Y. Gohar, M.A. Abdou
MACKLIB-IV, A Library of Nuclear Response Functions
Generated with the MACK-IV Computer Program from
ENDF/B-IV RSIC Data Library Collection
DLC-60 (1978)

/12/ R. Rühle, B. Riik: ISOSTO
IKE Bericht-Nr. 3-3.4.1177, 1972

/13/ M.B. Emmett: The MORSE Monte Carlo Radiation Transport
Code System
ORNL-4972 (1975)

/14/ Nuclear Engineering Handbook
McGraw Hill-Company, New York, 1958

/15/ W. Seelmann-Eggebert, G. Pfennig, H. Münzel
Nuklidkarte
Gesellschaft für Kernforschung mbH Karlsruhe, 1974

/16/ S. Glasstone, A. Sesonske
Nuclear Reactor Engineering
D. Van Nostrand Company, New York, 1963

/17/ Handbook of Chemistry and Physics
53rd edition 1972-1973, CRC-Press, p. B-94

/18/ G.I. Bell, S. Glasstone
Nuclear Reactor Theory
Van Nostrand Reinhold Company, New York, 1970

Appendix A

Calculation of Dancoff correction C

The Dancoff correction C is defined as the probability by which a neutron leaving a fuel region will reach another fuel region without any interaction. In our case of fuel plates with cladding and cooling gap this means that the neutron leaving the meat of one fuel plate has to travel through the cladding of this plate, then through the coolant and then through the cladding of the next fuel plate. So the Dancoff correction for a given direction Ω is

$$C\,(\Omega) = \exp-\{2*\Sigma_{cl} * l_{cl}(\Omega\,) + \Sigma_{gap} * l_{gap}(\Omega)\} \qquad (A.1)$$

The mean value C is given by integration of the entire angular space. To simplify the calculation of C, we assume that the mean value C can be got by integrating the value $li(\Omega)$. This leads to the mean rod length l_i, which is defined as $l_i=4V_i/S_i$ for zone i with V_i volume and S_i surface /18/.

So eq. (A.1) reads

$$C = \exp - \{2*\Sigma_{cl} * l_{cl} + \Sigma_{gap} * l_{gap}\} \qquad (A.2)$$

In the case of plates we can write

$$l_i = 2 * d_i \qquad (A.3)$$

with d_i the thickness of zone i.

So eq. (A.2) reads

$$C = \exp- \{4 * \Sigma_{cl} * d_{cl} + 2 * \Sigma_{gap}\ \ d*_{gap}\} \qquad (A.4)$$

The data for D_2O-cooled fuel plates are

$$d_{cl} = 0.033 \text{ cm}$$
$$d_{gap} = 0.2 \text{ cm}$$
$$\Sigma_{cl}\ (E=100\ \text{keV}) = 9 * 10^{-2}\ \text{cm}^{-1}$$
$$\Sigma_{gap} D_2O\ (E=100\ \text{keV}) = 0.3\ \text{cm}^{-1}$$

Using eq. (A.4) this leads to $C = 0.88$.